

**ABOUT THE USE OF FSO AND 58 GHZ MICROWAVE SYSTEMS
IN THE UMTS ACCESS NETWORK**

Luca Stroppolo

*Ericsson MUSEE – Advise / N&TC Transmission
Via Anagnina, 203 – 00118 Rome, Italy
luca.stroppolo@ericsson.com*

Abstract: Microwave access networks that backhaul UMTS nodes in urban areas are already quite dense in terms of links per square km. Since 2003, H3G started some investigations on Free Space Optics (FSO) and microwave equipment operating in the 58 GHz band as alternative solutions to traditional P-P links in less “crowded” spectrum environments. The proposed paper will analyse the major planning issues of these two technologies from the mobile operator point of view and envisage some possible applications. *Copyright © Ericsson/H3G*

Keywords: mobile backhauling, Free Space Optics, 58 GHz, laser communications

1. INTRODUCTION

The evolution of 3G services towards broadband demanding applications is requiring the mobile operator a constant increase in network capacity.

Urban microwave access networks that backhaul UMTS nodes to the core network are already quite dense in terms of links per square km (up to 4 links per square km) and spectrum occupancy (even at 38 GHz). Since each link affects the existent network in terms of interference level, any capacity upgrade requires a careful planning and remodelling of the access network, often slowing the planning and design process.

Since 2003, H3G started some investigations on Free Space Optics (FSO) and microwave equipment in the 58 GHz band as alternative solutions to traditional P-P urban links operating in less "crowded" spectrum environments.

The proposed paper will report the results of tests and measurements recorded on parallel links based on FSO and 58 GHz technologies.

Based on these trials, an analysis of the two technologies will carry on in terms of link availability, installation issues and propagation impairments, in the typical environment of an urban mobile network deployment.

2. TRIAL SET-UP

2.1 Environment description

In order to evaluate the two technologies in an environment eventually suited for their effective usage, an urban link based in Rome of about 780 m connecting a HUB site to a Node B, was chosen (see link profile in Fig. 1).

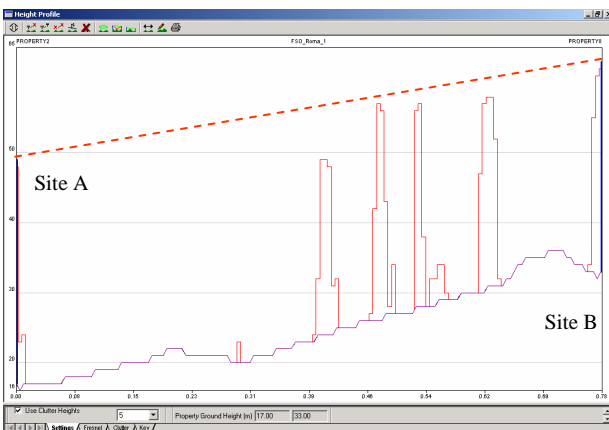


Fig. 1. Link profile

Site A is a tall office building of about 35 m height and site B is a building for residential location of about 25 m height, in full line-of-sight with site A.

2.2 Test bench description

The FSO system operating at 850 nm was provided by Alcatel and was commissioned on June 2003.

The test bench (see Fig. 2) was designed in order to collect received power level (AGC value every 100 ms), meteo data (visibility and rain intensity every minute) and error data (ES, SES and UAS) at E₁ base band interface for the go and return path (base band loop at remote end). A local PC, accessible both via the local network and remotely (via a dedicated RAS connection), collected these data.

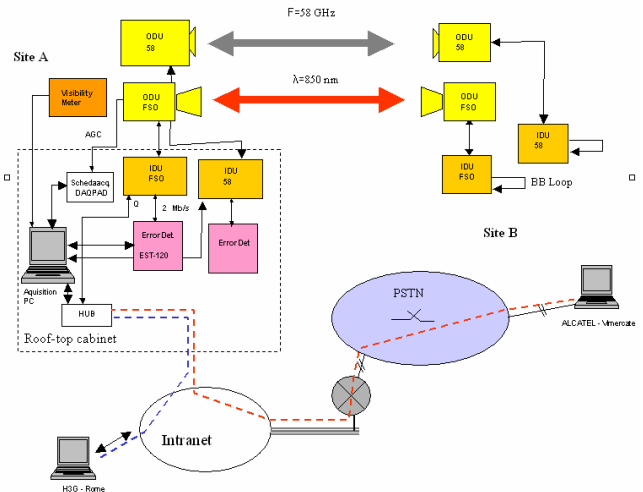


Fig. 2. FSO/58 GHz acquisition bench

On October 2004 a parallel link based on a 58 GHz PDH equipment, provided by Siemens, was installed between the same two sites.

Received power levels and radio performance (ES, SES, UAS) were collected via the Local Craft Terminal interface for both directions of the link, while an external error detector recorded error events at E₁ interface level for the go and return path.

Before installing the FSO and 58 GHz equipments many test and measurements were performed on the same equipment, in Alcatel and Siemens labs, in order to properly calibrate the test bench (AGC, receiver power level indications, transmitted power levels, receiver thresholds).

2.3 Acquisition periods

The acquisition period involved the FSO link from June 2003 up to March 2005, while the 58 GHz link was observed from October 2004 up to March 2005.

3. LINK PLANNING MODELS

3.1 FSO Link Budget Model

The design of the FSO link is nominally performed starting from the clear air propagation model in order to predict the nominal received power level and link

fade margin in the absence of fog, haze, rain, scintillations or other propagation impairments.

The received power is evaluated as:

$$P_{RXN} = P_{TX} + 20 \cdot \log_{10} \left(\frac{\phi_{RX}}{\theta} \right) - 20 \cdot \log_{10}(d) - L_p \quad (1)$$

Where: P_{RXN} [dBm] is the received power nominal level, d [km] is the length of the link, P_{TX} [dBm] is the transmitted power, θ [mrad] is the transmitter divergence, ϕ_{RX} [m] is the receiver diameter and L_p [dB] represents the pointing losses.

The divergence parameter takes into account the characteristics of the transmitter “directivity” and its typical value is of few mill radians.

It is easy to show that this parameter is equivalent to the antenna null-to-null microwave parabolic antenna aperture angle (in case of uniform field illumination), while the FSO receiver lens diameter is equivalent to the antenna diameter.

The clear air link budget model as in (1) is valid for $d > \phi_{RX}/\theta$ (for smaller distances the received power does not reduce with distance since the transmitted beam completely falls into the receiver aperture).

Table 1 reports the main FSO link parameters.

Table 1 FSO link budget

Operating wavelength	850	nm
Length	780	m
Transmitted Power	11	dBm
Receiver sensitivity (BER=10 ⁻⁶)	-47	dBm
Receiver diameter	10	cm
Transmitter divergence	3,40	mrad
Nominal Received Power Level (P_{RXN})	-20,5	dBm
Link Margin	26,5	dB

Transmitted power is intended measured after the transmitting lens system (true power of the beam in air) and the receiver threshold is intended included receiver telescope glass losses and the degradation due to ambient background light. It was also estimated a conservative value of pointing losses of about 3 dB.

In Fig. 3, the FSO power budget versus link distance is reported.

The vertical broken line intercepts the budget values for the actual trial link.

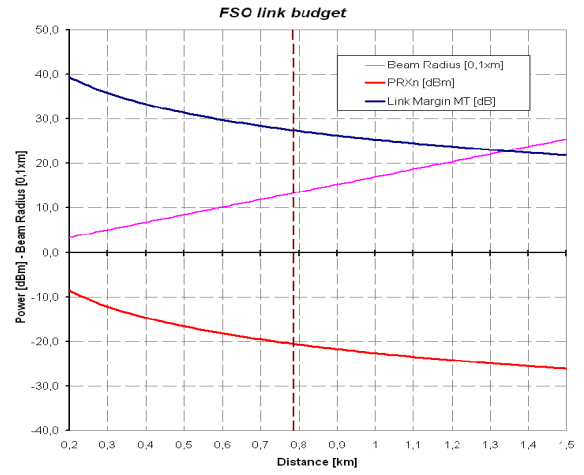


Fig. 3. FSO Link Budget

3.2 58 GHz Link Budget Model

The design of the 58 GHz link is performed in order to predict the reference received power level during clear air propagation.

The received power is evaluated as:

$$P_{RXN} = P_{TX} + G_A + G_B - 92,4 - 20 \cdot \log_{10}(F \cdot d) - \gamma_{O_2} \cdot d - L_p \quad (2)$$

Where: P_{RXN} [dBm], is the received power nominal level, d [km], is the length of the link, P_{TX} [dBm] is the transmitted power, G_A and G_B [dBi] are the antenna gains of the radio terminals, F [GHz] is the operating frequency, γ_{O_2} [dB/km] is the specific attenuation due to oxygen (see Fig. 4) and L_p [dB] represents the pointing losses.

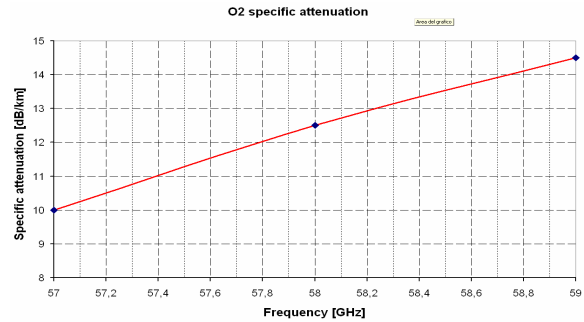


Fig. 4. O₂ specific attenuation

The model in Fig. 4 is intended for planning purposes and was obtained by some measurement tests performed at different frequencies in the 58 GHz band using the same calibrated bench used of the trial. Table 2 reports the main 58 GHz link parameters.

Table 2 - 58 GHz link budget

Frequency	57,975	GHz
Length	780	m
Transmitted power	7,4	dBm
Receiver sensitivity (BER=10 ⁻⁶)	-79,5	dBm
Polarization	V	
O2 attenuation	9,8	dB
Antenna gain (site A / site B)	34,0	dBi
Nominal Received Power Level (P_{RXN})	-61	dBm
Link Margin	18,6	dB

It was also estimated a conservative value of pointing losses of about 1 dB.

4. PROPAGATION IMPAIRMENTS

During the trial period the following propagation impairment (intended as additional attenuation with respect to P_{RXN}) were observed.

4.1 FOG attenuation

FSO link. Additional attenuation due to fog was the only impairment that caused link unavailability for the FSO link. These events are (as can be easily understood) very long in terms of service unavailability with respect to typical radio links downtimes due to rain. For instance, on 7 Dec 2003 unavailability of about 45 minutes was recorded and on 18 March 2004 the unavailability was of about 4 hours and 42 minutes.

In each of these cases additional attenuation overcame the measurement system dynamic range corresponding to specific attenuations of 45 dB/km.

Total FSO link unavailability due to fog was about 0,07 %, (99,93 % availability) in the period of observation.

Visibility is the meteorological parameter connected to fog additional specific attenuation γ_F via the following model:

$$\gamma_F = \frac{17}{V} \cdot \left(\frac{\lambda}{550} \right)^{-q} \quad [dB/km] \quad (3)$$

$$q = \begin{cases} 0 & V \leq 0.5 \quad km \\ V - 0.5 & 0.5 < V \leq 1 \quad km \\ 0.16 \cdot V + 0.34 & 1 < V \leq 6 \quad km \end{cases}$$

with $\lambda=850$ nm in considered link.

A comparison between this theoretical model and measured data for FSO links at 850 nm and 1550 nm is reported in (Mandich and Stroppolo, 2005).

Visibility statistics may be available from local sites (i.e. airports) and often published on the WEB. Anyway these statistics are not thought for FSO link planning; as a matter of fact they are generally averaged on 24 h period and for these purposes are not very useful. Anyway an interpolation model developed by Alcatel, in order to extend visibility statistics to different integration times, is proposed in (Mandich and Stroppolo, 2005)

Visibility and fog attenuation statistics recorded during the field trial period are reported in the following figures.

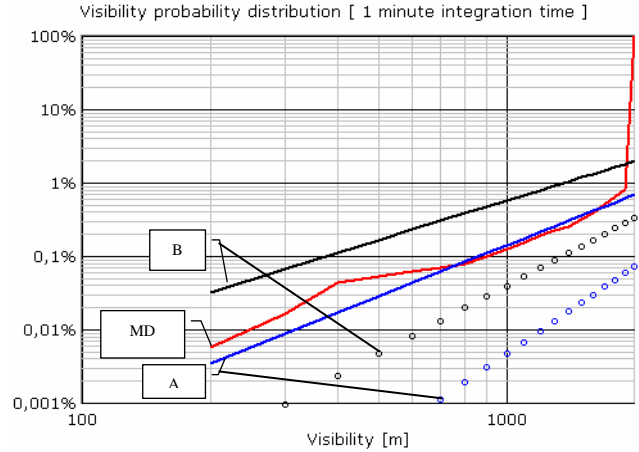


Fig. 6. Field trial visibility statistics (MD: measured data, 1 minute integration time)

In particular, Fig 6 reports Roma Urbe Airport, 24 h statistics (A dots) and its interpolated statistics to 3 h (A solid). Furthermore, Roma Fiumicino Airport at 24 h statistics (B dots) interpolated to 3h statistics (B solid) are shown.

Fig 7, reports the attenuation statistics measured during the trial (solid line) in addition with the prediction model derived from 3h interpolated statistics for Roma Urbe (dots above) and Roma Fiumicino (dots below). By the way, the FSO link happened to be deployed in the south part of the city of Rome, something in between Roma Urbe and Fiumicino.

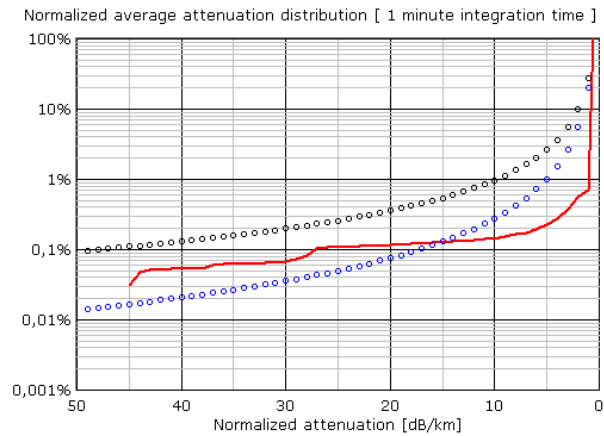


Fig. 7. Field Trial attenuation statistics (continuous line: measured data).

Taking into consideration the previous results, we can develop a simple model of the maximum distance (d_{MAX}) that can be performed by an FSO system of similar characteristics in terms of visibility occurrence due to fog and availability required by the link. See Table 3.

Table 3 – FSO maximum distance

Unavailability (availability %)	Visibility	d_{MAX}
≤ 30 minutes (99.994 %)	200 m	350 m
≤ 120 minutes (99.977 %)	300 m	500 m
≤ 240 minutes (99.954 %)	400 m	650 m

Since Table 3 is an extrapolation to very low occurrence statistics it should be intended only as an indication for the application of the FSO technology in an environment with meteorological statistics such as Rome. To this extent we can say that for such an environment, a generic FSO system can be used for carrier grade applications only for links not longer than about 300 m.

58 GHz link. No impact of haze or fog were observed to affect the 58 GHz link in the period considered for the measurement acquisition. This confirms what found in literature, with reported values of fog specific attenuation typically below 1 dB/km. See also (Bloom and Hartley, 2002).

4.2 Attenuation due to rain and snow

FSO link. For the period under measurement acquisition, specific attenuation due to rain was always below 20 dB/km,

Rain and attenuation data for the main severe rain events (about 40 recorded events) were grouped into rain interval and averaged. Events with rain intensity below 5 mm/h where discarded as well as rain events mixed with fog.

The following model:

$$\gamma = 1.45 \cdot R^{0.57} \quad [dB / km] \quad (4)$$

relating specific attenuation γ [dB/km] and rain intensity R [mm/h], seems to fit data with good correlation. Fig. 8 reports this model with some other models found in literature. Model 1 is found in (Bloom and Hartley, 2002) while Model 2 is found in (Carboneau and Wisely, 1998).

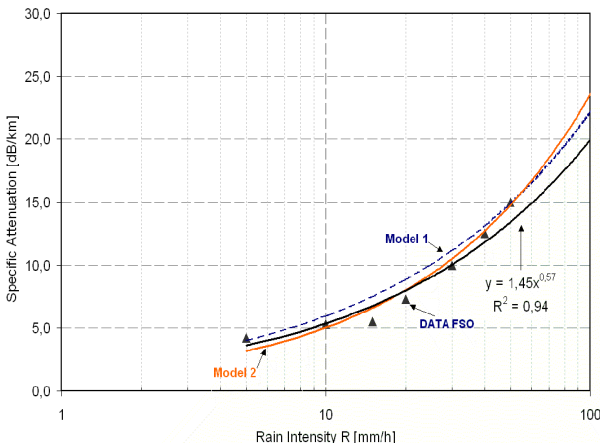


Fig. 8. FSO rain specific attenuation.

Based on model (4), some predictions can be made on the maximum length of an FSO in case of rain-limited operation. Considering an unavailability objective of 10 minutes per year due to rain and supposing a rain rate of R=50 mm/h at 0,01% of time assumed for the zone of Rome (something in between ITU-R Zones K and L), the maximum link distance is about 1.1 km. See Fig. 13.

The FSO link implemented for this trial had an estimated unavailability due to rain of about 2 minutes/year. Actually, no unavailability event caused by rain was recorded during the measurement period.

On the 23rd of January 2004 an atypical snow occurrence affected the south part of the city of Rome. The maximum attenuation recorded was about of 5 dB.

58 GHz link. Attenuation due to rain was the only significant impairment on the 58 GHz link, that was observed during the trial period. For that period, the link reported availability was of about 99.997%.

Fig. 9 reports the different behaviour of the 58 GHz link with respect to the FSO link in terms of attenuation induced by rain.

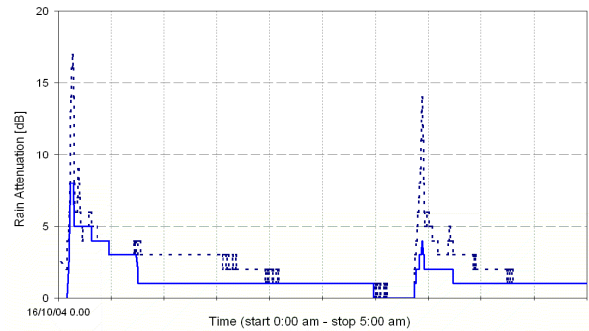


Fig. 9. Additional attenuation during a rain event (solid FSO, dotted 58 GHz).

The main rain events in the period of measurements recordings were analysed and the attenuation of FSO link and 58 GHz link compared (see scatter plot of Fig. 10).

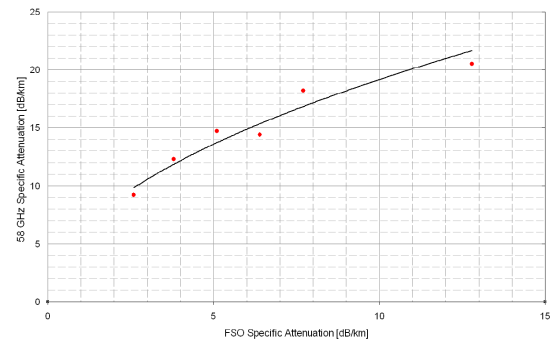


Fig. 10. 58 GHz link vs. FSO link specific rain attenuation.

Specific attenuation of the 58 GHz due to rain was confirmed to be greater than in the FSO case; the

trend line in the figure averages the behaviour between the two attenuations.

Some models relating specific attenuation at 58 GHz versus rain intensity can be found in literature. See Fig. 11.

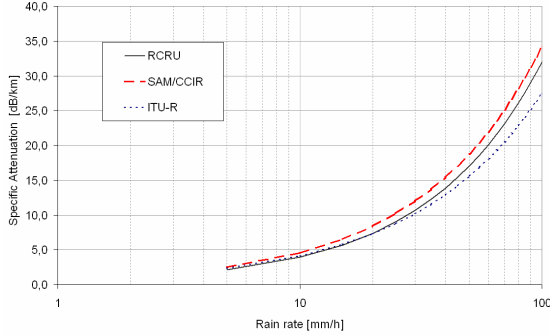


Fig. 11. Some 58 GHz link rain models.

The ITU-R model is taken from Rec. P.838-2 (dotted line).

The solid curve represents data excerpted from a publication of RCRU (Paulson and Gibbins, 2001). The one that seems to predict best the 58 GHz trial link availability performances is the Simplified Attenuation Model - SAM/CCIR that it is also the most conservative (broken line).

Using this model it is possible to estimate the maximum covered distance for this system being about 0,68 km in order to have 99,998% availability (10 minutes/year rain unavailability).

It was noted for the 58 GHz link that the measured specific attenuation versus rain intensity is higher with respect to the ITU-R propagation model. In order to clarify this issue, deeper investigations shall be undertaken and the installation of a second trial is under evaluation for a more comprehensive recording period and with an acquisition system having an extended dynamic range.

4.3 Scintillations

Local density fluctuations of the refractive index due to air turbulence may produce random variations of received power level around the mean value.

FSO link. Normally, for short FSO links, these fluctuations are of less importance with respect to attenuation due to fog/haze and rain. Moreover these links, if properly designed to countermeasure fog or rain, already satisfy required link margin for scintillation fades.

Nevertheless there could be some specific applications (i.e. long temporary links) where scintillations, added to other impairments, shall be taken into account as a limiting factor affecting the quality of the link.

For the duration of the measurements, the main scintillations activity occurred (as expected), during hottest summer days, with peak activity in the afternoon at 2:00 pm.

The model here adopted to describe the statistical fluctuations of the received power, is based on the well-known lognormal distribution. See for instance (Weichel, 1990) or (Biswas, 200).

$$P(F_s \geq F) = \frac{1}{2} \left\{ 1 + \operatorname{erf} \left[\sqrt{\frac{\sigma_i^2}{8}} \cdot \frac{\ln(10) \cdot F}{10 \cdot \sqrt{2 \cdot \sigma_i^2}} \right] \right\} \quad (5)$$

where F_s [dB] is the attenuation with respect the mean value of the received power level and σ_i^2 is the scintillation index. In practical applications, this value can be attained from measured received power level statistics. If field data are not available, σ_i^2 can be estimate from

$$\sigma_i^2 \cong 1.23 C_n^2 k^{\frac{7}{6}} d^{\frac{11}{6}} \left[1 + \frac{1.062 k \phi_{RX}^2}{4d} \right]^{\frac{7}{6}} \quad (6)$$

where k [m^{-1}] is the wave number, ϕ_{RX} [m] is the receiver aperture, d [m] is the link distance and C_n^2 [$m^{-2/3}$] the atmospheric structure.

Fig. 12 below shows a comparison between the scintillation model from (5) (dotted) and the measured one corresponding to a $C_n^2 = 8 \cdot 10^{-14} m^{-2/3}$ (solid).

The FSO link measured main scintillation activity in the period July-August 2003 with $C_n^2 = 1.2 \cdot 10^{-13} m^{-2/3}$, (medium high turbulence) corresponding to maximum attenuation of about 6 dB.

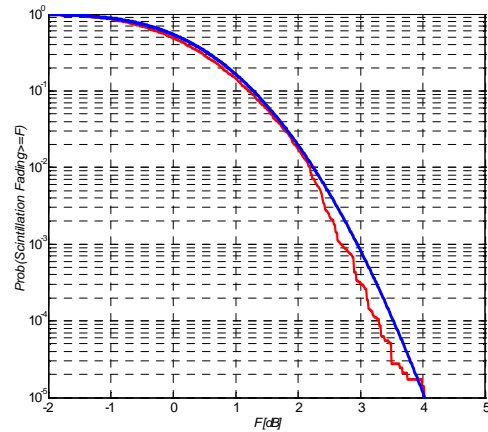


Fig. 12. Scintillation fading statistics

If it is assumed to consider the hottest part of a summer day (12:00 – 16.00 h) as the period of occurrence of strong scintillations (this was confirmed by field trial measurements), while tolerating just one deep fading per day exceeding the receiver threshold (i.e. 30 SES/month, for the hottest summer period), a maximum link length limited by scintillation can be estimated. For the system considered in this paper this length is approximately 1,8 km (see Fig. 13).

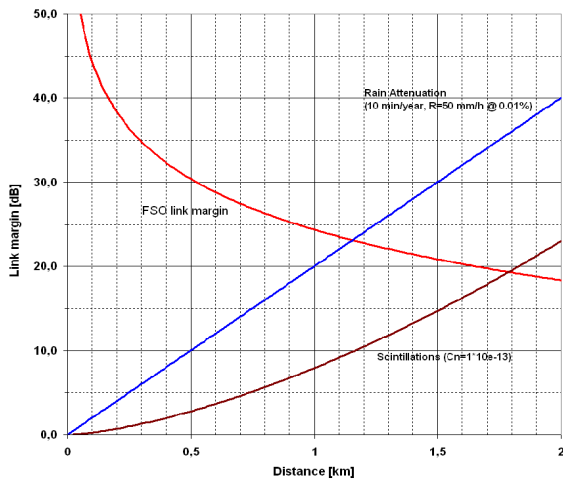


Fig. 13. FSO link distance (rainfall limited and scintillation limited)

58 GHz link. No significant scintillation effect was reported on the 58 GHz link. Small scintillation effects for these type of links, are probably within the tolerance of the measurement system and are not worse than in other microwave bands.

5. OTHER IMPAIRMENTS

Some other impairments on nominal receiver power level have been experienced during the trial period. These are significant for the FSO link only. Although not cause of any downtime by themselves, they should be accounted for the proper link planning.

5.1 Received power daily variations

Slow received power variation with diurnal periodicity were recorded on the FSO link. See Fig. 14.

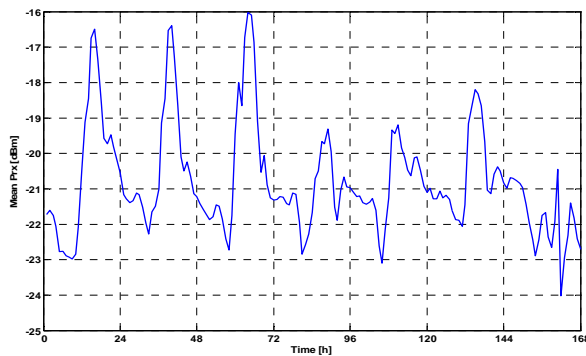


Fig. 14 – Received power diurnal variations (01/08/03 00:00 – 08/08/03 00:00)

It was noted that these variation are less marked during cloudy days. These variations were always within ± 4 dB with respect the nominal received power and never cause error events.

This behaviour seems to be typical for FSO links and could be explained considering that the receiver field of view of FSO systems (similar to the aperture angle for a microwave antenna) is typically of the order of some mrad. The trial system has about ± 2 mrad =

$\pm 0,1^\circ$ FoV while for the 58 GHz link the aperture angle at - 3 dB is about $\pm 1,2^\circ$.

In the present case, the site hosting the recorded FSO terminal is a tall rectangular building with the longest side exposed to the sun during most part of the day, while the opposite is left in the dark. Temperature gradients of the building could determine a slight periodical bending of the structure and a mispointing of the receiver terminal. As a matter of fact, power peaks of Fig.14 occur at about 4:00 pm each day (is the same hour when fine pointing of the link was completed during commissioning).

5.2 Average power long-term drift

A slow drift of the average received power level was observed on the FSO link with an overall degradation of about 5 dB from the time of installation (June 2003) to the end of the available recordings (March 2005).

5.3 Power fluctuations from wind flowing

In one occasion (14/11/04), fast received power variations afflicted the FSO link due to a strong wind flowing in the trial deployment area (up to 80 km/h as reported by some local weather stations).

Fig. 15 gives one-hour registration sample of the received power level at site A.

After this occurrence, the mean received power level never rose above -25 dBm confirming the need of a re-alignment of the link.

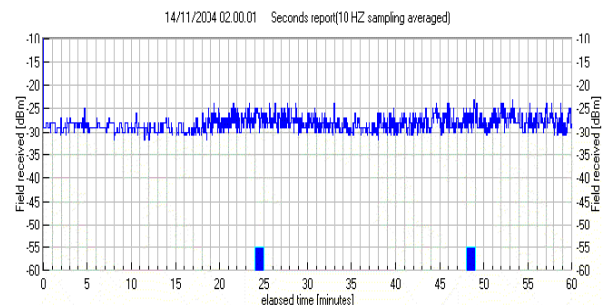


Fig. 15 – Received power during windstorm (14/11/2004 02:00 – 03:00 a.m.)

6. APPLICATIONS IN THE ACCESS NETWORK

It is not intention of this paper to give a final sharp assessment on both technologies, but simply report the experimental results from the field and analyse them from the mobile operator's perspective to find possible applications that match the needs of a fast growing access network, while maintaining carrier grade availability.

Trying to abstract from any particular equipment production, just keeping the focus on the general differences found in the behaviour of the FSO and 58 GHz link (mainly due to propagation and not on the specific equipment used), it is possible to say that:

- FSO systems are rain tolerant (up to 1.2 km) but fog is disrupting hence, if this is an issue for the

local environment, FSO are not suitable for carrier grade links. They do not require spectrum fee license and can be quickly deployed with no interference among systems. Attention is required in pointing properly the link (a skilled team is required). Mounting infrastructures require a certain level of rigidity and pointing needs periodical checks and realignments. No high/low distinction between outdoor units facilitates spare part management. FSO technology can be profitably used for temporary links (maximum length of the order of 2 km, limited by scintillations).

- 58 GHz links very similar to typical microwave ones. Rain is the affecting factor in order to fulfil operators requirement on availability so that limited distances must be addressed (below about 0.7 km). No particular requirements for installation and mounting infrastructure need to be considered and no particular attention must be paid for planning (small interference probability). 58 GHz systems may adopt TDD duplexing technique so synchronization should be performed on HUB installations. In Italy they still require spectrum fee license. 58 GHz systems can be profitably used in dense urban deployment, for very short links.

To lay these considerations into the transport section of a mobile network we can think of a typical hierarchical point-to-point architecture as reported in Fig. 16.

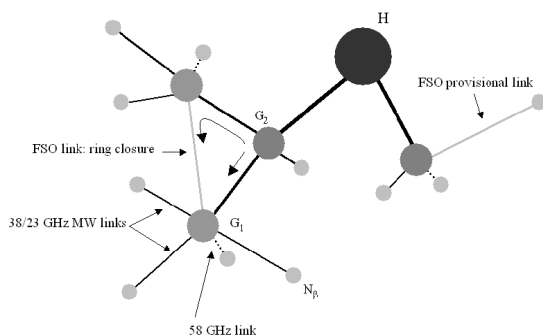


Fig. 16. Typical tree network architecture

The nodes N_{β} are the leaves of this structure and are backhauled to the transport network through different levels of grooming (i.e. G_1 and G_2). Each level is connected via point-to-point links of increasing capacity.

In a dense urban network deployment, more than 30% of the 38 GHz links serving the N_{β} could be implemented using 58 GHz band systems since their link distances are compatible with the limits imposed by rain attenuation at 58 GHz. On the contrary, less than about 5 % of these links would be compatible with distances allowed by an FSO system planned to give carrier grade availability in the presence of fog. Anyhow, FSO systems could be used for “long” provisional links when a quick deployment is required. Another potential use of FSO technology

could be foreseen when a further degree of protection is needed to be introduced at grooming level. In this case the FSO link can be used as a closing side of a “SNCP like” ring with the other sides already implemented with traditional microwave links.

6. SUMMARY AND CONCLUSIONS

This paper presented the main field results acquired from two parallel links based on FSO and 58 GHz technologies. These data were analysed with particular regards to propagation impairments, design and planning issues from the mobile operator’s perspective, to find possible applications that match the needs of a fast capacity growing access network, while maintaining carrier grade availability.

FSO link are more rain tolerant but, if fog is an issue for the local environment, they are not suitable to provide carrier grade availabilities. In any case some minor applications, in this perspective, can be found when provisional links are needed or in synergy with the existing architecture to increase network protection.

58 GHz links are rain limited and behave much more likely microwave links in other “traditional” frequency bands; they don’t need any particular attention in planning and commissioning and can be profitably used to connect edge nodes at short distances.

Finally both technologies are suitable for crowded deployments since for them interferences are not an issue.

6. ACKNOWLEDGEMENTS

The author wishes to thank all staff from (formerly) Alcatel and (formerly) Siemens that greatly contributed to the deployment and the execution of the trials. Special thanks to Mr. D. Mandich, Mr. G. Paoli, Mrs. E. Grassi, Mr. W. Manna, Mr. R. Milani, Mr. M. Spairani, Mr. S. Petrachi, Mr. C. Bolzoni.

REFERENCES

- Mandich, D., L. Stroppolo (2005). A complete propagation model for FSO applications and a comparison with measured data. ECPS 2005 Conference, Brest, France.
- Bloom, S., W. S. Hartley (2002). Hybrid FSO Radio (HFR): Some Preliminary Results. *Optical Wireless Communications V*, pp 143-154, Eric J. Korevar Editor, proceedings of SPIE **Volume 4873**, Boston, USA.
- Carbonneau, T. H., D.R. Wisely (1998) Opportunities and challenges for optical wireless; the competitive advantage of free space telecommunications link in today’s crowded market place. SPIE Conference on optical

- wireless communications, 1998, **Volume 3232**, Boston, Massachusetts, USA.
- Paulson, K. S., C. J. Gibbins (2001) Report on Analysis of 500 m range data. Radio Communications Research Unit, Rutherford Appleton Laboratory, Chilton, Oxfordshire, UK.
- Weichel, H. (1990) *Laser Beam propagation in the Atmosphere*, chapter 5, **Volume TT3**, Tutorial Texts in Optical Engineering, Roy F. Potter, Series Editor, SPIE Optical Engineering Press, Washington, USA
- Biswas, S. Lee (2000), Ground-to-Ground Optical Communications Demonstration, TMO Progress Report 42-141

BIOGRAPHY



Luca Stroppolo received his master degree in Electronic Engineering from the II University of Rome Tor Vergata in 1993. From the beginning of 1995 to 2001 he was at the Network Engineering department of Telecom

Italia where he was involved with the specifications and system analysis of wireless systems (Point to Multipoint systems and Wireless LAN), including testing and field trials. By that time he was also a member of ETSI TM4 standardization group.

From 2001 to 2002 he was at Edisontel as responsible for the deployment of the radio access network and from 2002 to 2005 he was at 3 Italia in the Radio Network Planning department involved with microwave radio link design and system engineering. From 2006 he works at Ericsson Market Unit South East Europe (MUSEE) Service/Advise, responsible for the Microwave Engineering section and is involved with the design of microwave networks, access network planning and microwave system engineering.